

Effects of interface bound states on the shot noise in normal metal-low-dimensional Rashba semiconductor tunnel junctions with induced s-wave pairing potential

Wen-Xiang Chen(陈文祥), Rui-Qiang Wang(王瑞强), Liang-Bin Hu(胡梁宾)

Citation: Chin. Phys. B . 2019, 28(5): 057201. **doi:** 10.1088/1674-1056/28/5/057201
Journal homepage: http://cpb.iphy.ac.cn; http://iopscience.iop.org/cpb

What follows is a list of articles you may be interested in

Inverse spin Hall effect in ITO/YIG exited by spin pumping and spin Seebeck experiments

Kejian Zhu(朱科建), Weijian Lin(林伟坚), Yangtao Su(苏仰涛), Haibin Shi(石海滨), Yang Meng(孟洋), Hongwu Zhao(赵宏武)

Chin. Phys. B . 2019, 28(1): 017201. **doi:** 10.1088/1674-1056/28/1/017201

Influence of spin-orbit coupling on spin-polarized electronic transport in magnetic semiconductor nanowires with nanosized sharp domain walls

Lian Liu(刘恋), Wen-Xiang Chen(陈文祥), Rui-Qiang Wang(王瑞强), Liang-Bin Hu(胡梁宾)

Chin. Phys. B . 2018, 27(4): 047201. **doi:** 10.1088/1674-1056/27/4/047201

Unified semiclassical approach to electronic transport from diffusive to ballistic regimes

Hao Geng(耿浩), Wei-Yin Deng(邓伟胤), Yue-Jiao Ren(任月皎), Li Sheng(盛利), Ding-Yu Xing(邢定钰)

Chin. Phys. B . 2016, 25(9): 097201. **doi:** 10.1088/1674-1056/25/9/097201

Tunneling magnetoresistance based on a Cr/graphene/Cr magnetotunnel junction

Luan Gui-Ping, Zhang Pei-Ran, Jiao Na, Sun Li-Zhong

Chin. Phys. B . 2015, 24(11): 117201. **doi:** 10.1088/1674-1056/24/11/117201

Spin-dependent negative differential conductance in transport through single-molecule magnets

Luo Wei, Wang Rui-Qiang, Hu Liang-Bin, Yang Mou

Chin. Phys. B . 2013, 22(4): 047201. **doi:** 10.1088/1674-1056/22/4/047201

Effects of interface bound states on the shot noise in normal metal–low-dimensional Rashba semiconductor tunnel junctions with induced s-wave pairing potential

Wen-Xiang Chen(陈文祥), Rui-Qiang Wang(王瑞强), and Liang-Bin Hu(胡梁宾)†

Guangdong Provincial Key Laboratory of Quantum Engineering and Quantum Materials, School of Physics and Telecommunication Engineering, South China Normal University, Guangzhou 510631, *China*

(Received 16 December 2018; revised manuscript received 24 January 2019; published online 4 April 2019)

We consider the effects of interface bound states on the electrical shot noise in tunnel junctions formed between normal metals and one-dimensional (1D) or two-dimensional (2D) Rashba semiconductors with proximity-induced s-wave pairing potential. We investigate how the shot noise properties vary as the interface bound state is evolved from a non-zero energy bound state to a zero-energy bound state. We show that in both 1D and 2D tunnel junctions, the ratio of the noise power to the charge current in the vicinity of zero bias voltage may be enhanced significantly due to the induction of the midgap interface bound state. But as the interface bound state evolves from a non-zero energy bound state to a zero-energy bound state, this ratio tends to vanish completely at zero bias voltage in 1D tunnel junctions, while in 2D tunnel junctions it decreases smoothly to the usual classical Schottky value for the normal state. Some other important aspects of the shot noise properties in such tunnel junctions are also clarified.

Keywords: interface bound state, tunnel junction, shot noise

PACS: 72.10.Bg, 72.25.Dc, 72.25.Ba, 72.15.–v **DOI:** 10.1088/1674-1056/28/5/057201

1. Introduction

In recent years, the exploitation of spin–orbit coupling as a way to achieve a spin-dependent coupling to the superconducting state has attracted much theoretical and experimental interest. Within this context, a number of interesting phenomena have been predicted, such as spin manipulation based on spin-polarized supercurrent,[1–4] magneto-anisotropic Josephson effect,[5] anisotropic and paramagnetic Meissner effect,[6] spin-galvanic couplings,[7] etc.[8,9] An interesting way of achieving this spin-dependent coupling is by means of superconductor-proximity effect in low-dimensional semiconductor heterostructures with strong spin–orbit interaction.[10–16] In these heterostructures, the Cooper pairing potential in a superconductor can penetrate into a proximity-coupled semiconductor nanowire or thin film with strong spin–orbit interaction, and the interplay of the proximity-induced Cooper pairing potential and the intrinsic spin–orbit coupling can lead to the formation of a helical superconducting state in the semiconductor. An interesting property of these helical superconducting states is that they can host anomalous edge bound states in the presence of a Zeeman magnetic field, which may manifest as chiral Andreev bound states or even chiral Majorana zero-energy modes under some particular conditions.[10–16] The transition from chiral Andreev bound states to chiral Majorana zero-energy modes can be realized by tuning some relevant physical parameters, such as the strength of the applied Zeeman magnetic field. Since these chiral Majorana zero-energy modes are promising for future applications in quantum computation, the studies of various properties of such anomalous edge states are of interest from both theoretical and practical points of view. Among these studies, a fundamental issue is how to detect such anomalous edge states or how to identify unambiguously their true nature. The simplest way to detect such anomalous edge states is by the measurement of the tunneling conductance spectroscopy. The theoretical analyses predict that, if a zero-energy bound state is formed at the edges of a semiconductor nanowire (or thin film) with proximity-induced s-wave pairing potential, then the differential tunneling conductance spectrum of electrical transport from a normal lead to such a semiconductor will exhibit a conductance peak at zero bias voltage, similar to other zero-energy bound states in superconductors.[17,18] Thus, the observation of zero-bias conductance peaks (ZBCPs) in the tunneling conductance spectroscopy can serve as an important signature of the possible presence of a chiral Majorana zero-energy mode. These ZBCPs have indeed been experimentally observed in recent measurements of the tunneling conductance spectra in semiconductor nanowires (both InSb and InAs) with proximity-induced superconductivity.[19–25] However, from the theoretical point of view, the observation of such ZBCPs in the tunneling conductance spectrum represents only a necessary but not a sufficient evidence for the possible presence of chiral Majorana zero-energy mode. The main problem with the unambiguous identification of the true nature of such ZBCPs is that there are some other sources that may also lead to the occurrence of similar ZBCPs in the tunneling conductance spectrum

†Corresponding author. E-mail: lbhu26@126.com

© 2019 Chinese Physical Society and IOP Publishing Ltd

of such systems.[26–28] Due to these complexities, more possible signatures should be searched to unambiguously identify the true nature of these ZBCPs.

In this paper, we consider the effects of anomalous interface bound states on the electrical shot noise in tunnel junctions formed between normal metals and low-dimensional semiconductors with strong Rashba spin–orbit coupling and proximity-induced s-wave Cooper pairing potential. The electrical shot noise originates from the time-dependent fluctuation of the electric current in electrical transport due to the discreteness of the charge of the carriers. It is known that shot noise measurements can provide some useful information on the transport process in a system, which is not available through usual conductance measurements.[29–36] For example, it can help to obtain information on the charge and statistics of the quasiparticles relevant for electrical transport in a system and reveal information on the internal energy scales of a low-dimensional system. In the zero-temperature limit, shot noise remains as the only source of electric noise. In normal metallic conductors, the process of electrical conductance can be modeled by a Poisson process in the absence of correlations among the carriers, then one can show that for small bias voltage, the ratio of the noise power to the electric current will equal to $2e$ in the zero-temperature limit.[29] The dissipationless current (supercurrent) in superconductors is a property of the ground state, and therefore is noiseless. However, noise appears if the superconductor is in contact with normal metals. It has been predicted that in the low transmission normal metal–superconductor junctions, due to the transport of Cooper pairs (charged $2e$) in the superconductor region, the ratio of the noise power to the electric current will be doubled with respect to the normal-state result $2e$.[29,30] But if interface bound states emerge in a tunnel junction, then the result may be altered significantly.[31,32] At this stage, it is important to clarify what influences the anomalous interface bound states might have on the electrical shot noise in tunnel junctions formed between normal metals and low-dimensional semiconductors with strong Rashba spin–orbit coupling, proximity-induced s-wave Cooper pairing potential, and Zeeman magnetic field. It should be pointed out that in tunnel junctions with only normal electronic states involved, the formation of interface bound states may also have significantly influence the shot noise properties of the junctions; as was found, for example, in Fe|MgO|Fe magnetic tunnel junctions.[36] Compared with tunnel junctions with only normal states involved, in tunnel junctions of low-dimensional semiconductors with strong spin–orbit coupling and proximity-induced s-wave pairing potential, some new physics may occur due to the following reasons. First, in these tunnel junctions, the formation of interface bound states is not a pure boundary effect but results from the interplay of boundary effect, strong spin–orbit coupling, proximity-induced Cooper pairing potential, and applied Zeeman magnetic field. Second, in these tunnel junctions, due to the formation of helical superconducting states in the junctions, Andreev reflection plays a very important role on charge transmission through the interfaces, it may especially play a dominant role in the gap region. Due to the combined effects of these complex factors, the influences of the interface bound states on the shot noise in such tunnel junctions may exhibit some unusual characteristics. In this paper, based on the extended Landauer–Büttiker scattering theory,[29–32] we will investigate in some detail what can be expected in the electrical shot noise in these tunnel junctions under the presence of anomalous interface bound states. We are particularly interested in how the electrical shot noise properties vary as the interface bound state is evolved from a non-zero energy bound state to a zero-energy bound state. We will show that, because this evolution is driven by tuning the strength of the applied Zeeman magnetic field, the electrical shot noise in such tunnel junctions may exhibit some interesting behaviors. The observation of such interesting behaviors may provide some useful information on the properties of anomalous interface bound states formed in such low-dimensional systems, which cannot be obtained by usual conductance measurements.

This paper is organized as follows. In Section 2, we describe the theoretical model for the systems considered in the paper and introduce the theoretical formulation for the calculation of the electrical shot noise. In Section 3, we numerically calculate the shot noise as a function of some relevant physical parameters. We will discuss in some detail how the shot noise properties vary as the interface bound state evolves from a non-zero energy bound state to a zero-energy bound state.

2. Model and formulation

We consider the electrical shot noise of the interface between a normal metal and a one-dimensional (1D) or two-dimensional (2D) semiconductor with strong Rashba spin–orbit coupling (such as InSb or InAs nanowires or thin films) and proximity-induced s-wave pairing potential. When the superconducting region in such a tunnel junction is subjected to a Zeeman magnetic field in the direction perpendicular to the Rashba field, the Andreev bound states will emerge at the interfaces in both 1D and 2D systems. Below we take 2D tunnel junctions as the example to discuss how to calculate the electrical shot noise of the interfaces. The shot noise in the 1D tunnel junctions can be calculated in a similar way.

A 2D Rashba semiconductor with proximity-induced s-wave pairing potential and subjected to a Zeeman magnetic field in the direction perpendicular to the Rashba field can be described by the following Bogliubov–de Gennes (BdG) Hamiltonian:

$$H = \begin{pmatrix} H_0(\boldsymbol{k},\sigma) & \mathrm{i}\sigma_y\Delta \\ -\mathrm{i}\sigma_y\Delta & -H_0(-\boldsymbol{k},\sigma^*) \end{pmatrix}, \tag{1}$$

where $\sigma=(\sigma_x,\sigma_y,\sigma_z)$ are the Pauli matrices in spin space, Δ is the proximity-induced s-wave pairing potential, $H_0(\boldsymbol{k},\sigma)$ is the effective Hamiltonian describing the normal state of the 2D Rashba semiconductor

$$H_0(\boldsymbol{k},\sigma)=\xi_{\boldsymbol{k}}+\alpha_{\rm R}(\sigma_x k_y-\sigma_y k_x)+B_0\sigma_z, \tag{2}$$

where $\xi_{\boldsymbol{k}}=\hbar^2\boldsymbol{k}^2/2m_{\rm s}-\mu_{\rm s}$ is the kinetic energy relative to the chemical potential $\mu_{\rm s}$, $\boldsymbol{k}=(k_x,k_y)$ is the two-dimensional wave vector, $m_{\rm s}$ is the effective mass, $\alpha_{\rm R}$ is the Rashba spin–orbit coupling constant, and B_0 is the strength of the applied Zeeman magnetic field.

By solving the BdG equation, the eigenvalues of quasiparticles in the superconducting region are given by

$$\begin{aligned}&E_{{\rm e},\pm}(k_x,k_y)\\&=\sqrt{\xi_{\boldsymbol{k}}^2+\alpha_{\rm R}^2k^2+B_0^2+\Delta^2\pm2\sqrt{B_0^2\Delta^2+B_0^2\xi_{\boldsymbol{k}}^2+\alpha_{\rm R}^2k^2\xi_{\boldsymbol{k}}^2}},\end{aligned} \tag{3}$$

$$\begin{aligned}&E_{{\rm h},\pm}(k_x,k_y)\\&=-\sqrt{\xi_{\boldsymbol{k}}^2+\alpha_{\rm R}^2k^2+B_0^2+\Delta^2\pm2\sqrt{B_0^2\Delta^2+B_0^2\xi_{\boldsymbol{k}}^2+\alpha_{\rm R}^2k^2\xi_{\boldsymbol{k}}^2}},\end{aligned} \tag{4}$$

in which $k=\sqrt{k_x^2+k_y^2}$. The dispersion relations of electron-like and hole-like quasiparticles in the superconducting region are determined by Eqs. (3) and (4), respectively. The corresponding eigenvectors of quasiparticles can also be obtained analytically.

Now we consider the reflection and transmission of charge carriers at the interface between the normal lead and the superconducting region. We assume that the interface is located at $x=0$ and has an infinitely narrow insulating barrier described by the δ function: $U(x)=U_0\delta(x)$, with the interface barrier strength U_0. We denote the spinor eigenvectors (in Nambu space) of electrons (e) or holes (h) in the normal lead as $|\sigma\rangle_{\rm e,h}$, with $\sigma=+$ for spin up and $\sigma=-$ for spin down. Then, for an electron of spin σ incident from the normal lead, the wave function in the normal lead can be expressed as

$$\begin{aligned}\Psi(x<0)\;=\;&{\rm e}^{{\rm i}k_y y}[{\rm e}^{{\rm i}k_x^{({\rm e})}x}|\sigma\rangle_{\rm e}+a_{\sigma\sigma}{\rm e}^{{\rm i}k_x^{({\rm h})}x}|\sigma\rangle_{\rm h}\\&+a_{\sigma\bar\sigma}{\rm e}^{{\rm i}k_x^{({\rm h})}x}|\bar\sigma\rangle_{\rm h}+b_{\sigma\sigma}{\rm e}^{-{\rm i}k_x^{({\rm e})}x}|\sigma\rangle_{\rm e}\\&+b_{\sigma\bar\sigma}{\rm e}^{-{\rm i}k_x^{({\rm e})}x}|\bar\sigma\rangle_{\rm e}].\end{aligned} \tag{5}$$

Here $a_{\sigma\sigma}$ and $a_{\sigma\bar\sigma}$ are the Andreev reflection coefficients of an incident electron with spin σ reflected to a hole with spin σ or $\bar\sigma$ ($\bar\sigma=-\sigma$), $b_{\sigma\sigma}$ and $b_{\sigma\bar\sigma}$ are the normal reflection coefficients of an incident electron with spin σ reflected to an electron with spin σ or $\bar\sigma$. k_y is the y component of the wave vectors of the incident electrons, which is a conserved quantity during the reflection and the transmission processes. $k_x^{({\rm e})}$ and $k_x^{({\rm h})}$ are the x components of the wave vectors of reflected electrons and holes, respectively, with $k_x^{({\rm e})}=\sqrt{(2m_{\rm N}/\hbar^2)(E+\mu_{\rm N})-k_y^2}$ and $k_x^{({\rm h})}=\sqrt{(2m_{\rm N}/\hbar^2)(\mu_{\rm N}-E)-k_y^2}$, in which $\mu_{\rm N}$ is the chemical potential and $m_{\rm N}$ is the effective mass in the normal lead.

The wave function of the scattering state in the superconducting region is given by

$$\psi(x>0)=\sum_{n=1}^{4}c_n{\rm e}^{{\rm i}q_n x}{\rm e}^{{\rm i}k_y y}\varphi(q_n,k_y). \tag{6}$$

Here the coefficients c_n denote the amplitudes of quasiparticles propagating in the superconducting region, q_n denotes the x component of the wave vectors of the quasiparticles, $\varphi(q_n,k_y)$ denotes the corresponding spinor eigenvector of the quasiparticles with the wave vector (q_n,k_y), which can be obtained by solving the BdG equation.

When the energy E and the y component k_y of the wave vector of an incident electron (or hole) are given, the wave number q_n in Eq. (6) can be determined self-consistently from the energy dispersion relations of quasiparticles in the superconducting region, given by Eq. (3) (for electron-like quasiparticles) or Eq. (4) (for hole-like quasiparticles). In general, one can obtain eight solutions for q_n from the energy dispersion relations of quasiparticles when E and k_y are given. If the solution of q_n is a real number, the corresponding wave function represents a propagating wave. If q_n is a complex number, then the corresponding wave function represents an evanescent wave. In general, the solution of q_n is a complex number. Since we have assumed that quasiparticles are transmitted from the region of $x<0$ to the region of $x>0$, in the determination of the solution for q_n, the constraints $\partial E_{{\rm e},\pm}(q_n,k_y)/\partial q_n>0$ (for electron-like quasiparticles) and $\partial E_{{\rm h},\pm}(q_n,k_y)/\partial q_n>0$ (for hole-like quasiparticles) should be postulated for propagating waves and the constraint ${\rm Im}(q_n)>0$ should be postulated for evanescent waves. After imposing these constraints, the values of the four wave numbers q_n in Eq. (6) can be determined uniquely from the energy dispersion relation of quasiparticles by setting $E_{{\rm e},\pm}(q_n,k_y)=E$ (for $E>0$) or $E_{{\rm h},\pm}(q_n,k_y)=E$ (for $E<0$) when E and k_y are given. After the values of the four wave numbers q_n are determined, the corresponding spinor eigenvectors, denoted as $\varphi(q_n,k_y)\equiv[u_\uparrow(q_n,k_y),u_\downarrow(q_n,k_y),v_\uparrow(q_n,k_y),v_\downarrow(q_n,k_y)]^{\rm T}$, can also be obtained from the BdG equation, with

$$\begin{aligned}&u_\uparrow(q_n,k_y)\\&=-\frac{1}{N(q_n,k_y)}\frac{2{\rm i}\alpha_{\rm R}(q_n-{\rm i}k_y)(\xi_{q_n,k_y}-B_0)}{\Delta},\end{aligned} \tag{7}$$

$$\begin{aligned}&u_\downarrow(q_n,k_y)\\&=\frac{1}{N(q_n,k_y)}\frac{\Delta^2+\xi_{q_n,k_y}^2+\alpha_{\rm R}^2(q_n^2+k_y^2)-(B_0-E)^2}{\Delta},\\&v_\uparrow(q_n,k_y)\end{aligned} \tag{8}$$

$$= \frac{1}{N(q_n,k_y)}\left[\frac{(\xi_{q_n,k_y}-B_0-E)}{\Delta}u_\downarrow - \frac{\mathrm{i}\alpha_\mathrm{R}(q_n+\mathrm{i}k_y)}{\Delta}u_\uparrow\right], \quad (9)$$

$$v_\downarrow(q_n,k_y)$$

$$= \frac{-1}{N(q_n,k_y)}\left[\frac{(\xi_{q_n,k_y}+B_0-E)}{\Delta}u_\uparrow + \frac{\mathrm{i}\alpha_\mathrm{R}(q_n-\mathrm{i}k_y)}{\Delta}u_\downarrow\right], \quad (10)$$

where $\xi_{q_n,k_y}=\hbar^2(q_n^2+k_y^2)/2m-\mu_\mathrm{s}$ and $N(q_n,k_y)$ is a normalization factor.

At the interface between the normal lead and the superconducting region, the matching conditions for the wave functions are

$$\Psi|_{x=0^-}=\Psi|_{x=0^+}, \quad (11)$$

$$\hat{V}^{(\mathrm{N})}\Psi|_{x=0^-}=\hat{V}^{(\mathrm{S})}\Psi|_{x=0^+}-\frac{\hbar}{m\mathrm{i}}\frac{2mU_0}{\hbar^2}(\sigma_0\otimes\tau_z)\Psi|_{x=0^+}, \quad (12)$$

where $\hat{V}^{(\mathrm{N})}$ is the velocity operator in the normal lead, $\hat{V}^{(\mathrm{S})}$ is the velocity operator in the superconducting region, σ_0 is the unit matrix in spin space, and τ_z is the Pauli matrix in particle–hole space. By solving Eqs. (11) and (12), for an incident electron with energy E and incident angle θ (defined by $k_y=k\sin\theta$), the normal and the Andreev reflection coefficients $b_{\sigma\sigma'}$ and $a_{\sigma\sigma'}$ in Eq. (5) can be calculated, which are the functions of the incident energy E and the incident angle θ. In the following, we will use $R^\mathrm{e}_{\sigma\sigma'}$ to denote the normal reflection probability of an incident electron with spin σ reflected to an electron with spin σ', and use $R^\mathrm{h}_{\sigma\sigma'}$ to denote the Andreev reflection probability of an incident electron with spin σ reflected to a hole with spin σ'. In terms of the normal and the Andreev reflection coefficients $b_{\sigma\sigma'}$ and $a_{\sigma\sigma'}$, the normal and the Andreev reflection probabilities of an incident electron with energy E and incident angle θ and spin σ are given by

$$R^\mathrm{e}_{\sigma\sigma'}=|b_{\sigma\sigma'}(E,\theta)|^2, \quad R^\mathrm{h}_{\sigma\sigma'}=\frac{k_x^{(\mathrm{h})}}{k_x^{(\mathrm{e})}}|a_{\sigma\sigma'}(E,\theta)|^2, \quad (13)$$

which are the functions of the incident energy E and the incident angle θ.

After the normal and the Andreev reflection probabilities are obtained, the average electric current and the fluctuation around the average electric current (i.e., the shot noise) can be obtained following the extended Landauer–Büttiker scattering theory.[29–32] In the zero-temperature limit, the average electric current at a bias voltage V is given by

$$I=\frac{1}{e}\int_0^{eV}G(E)\,\mathrm{d}E, \quad (14)$$

where $G(E)$ is the differential tunneling conductance at zero-temperature, which can be expressed as an integration over the incident angle θ of the incident electrons as follows:

$$G(E) = \frac{\mathrm{e}^2}{h}\sum_\sigma\frac{1}{2}\int_{-\pi/2}^{\pi/2}\left[1+R^\mathrm{h}_{\sigma\sigma}+R^\mathrm{h}_{\sigma\bar{\sigma}} - R^\mathrm{e}_{\sigma\sigma}-R^\mathrm{e}_{\sigma\bar{\sigma}}\right]\times\cos\theta\,\mathrm{d}\theta. \quad (15)$$

In the zero-temperature limit, the shot-noise power at bias voltage V is given by

$$P=\frac{1}{e}\int_0^{\mathrm{eV}}S(E)\,\mathrm{d}E, \quad (16)$$

where $S(E)$ is the differential shot noise at zero-temperature, which can also be expressed as an integration over the incident angle θ of the incident electrons as follows:

$$S(E)=\frac{2\mathrm{e}^3}{h}\sum_\sigma\frac{1}{2}\int_{-\pi/2}^{\pi/2}s_\sigma(E,\theta)\times\cos\theta\,\mathrm{d}\theta, \quad (17)$$

where $s_\sigma(E,\theta)$ is the function of the energy E and the incident angle θ of the incident electrons with spin σ and is given by the normal and the Andreev reflection probabilities as follows:

$$\begin{aligned}s_\sigma(E,\theta) = {} & R^\mathrm{e}_{\sigma\sigma}(1-R^\mathrm{e}_{\sigma\sigma})+R^\mathrm{e}_{\sigma\bar{\sigma}}(1-R^\mathrm{e}_{\sigma\bar{\sigma}}) \\ & +R^\mathrm{h}_{\sigma\sigma}(1-R^\mathrm{h}_{\sigma\sigma})+R^\mathrm{h}_{\sigma\bar{\sigma}}(1-R^\mathrm{h}_{\sigma\bar{\sigma}})+2R^\mathrm{e}_{\sigma\sigma}R^\mathrm{e}_{\sigma\bar{\sigma}} \\ & +2R^\mathrm{h}_{\sigma\sigma}R^\mathrm{h}_{\sigma\bar{\sigma}}+2(R^\mathrm{e}_{\sigma\sigma}+R^\mathrm{e}_{\sigma\bar{\sigma}})(R^\mathrm{h}_{\sigma\sigma}+R^\mathrm{h}_{\sigma\bar{\sigma}}). \quad (18)\end{aligned}$$

3. Results and discussion

In this section, we present some numerical results obtained using the theoretical formulation introduced above. We will investigate in some detail how the electrical shot noise properties vary as the interface bound state is evolved from a non-zero energy bound state to a zero-energy bound state in both 1D and 2D tunnel junctions. For convenience of discussion, we use dimensionless parameters in the numerical results presented below. We define the strength of the interface barrier by a dimensionless parameter $Z_0\equiv 2m_\mathrm{s}U_0/\hbar^2k_\mathrm{F}^{(\mathrm{s})}$ and the strength of the Rashba spin–orbit coupling by a dimensionless parameter $\alpha\equiv 2m_\mathrm{s}\alpha_\mathrm{R}/\hbar^2k_\mathrm{F}^{(\mathrm{s})}$, where $k_\mathrm{F}^{(\mathrm{s})}=\sqrt{2m_\mathrm{s}\mu_\mathrm{s}/\hbar^2}$ is the Fermi wave number in the superconducting region. The pairing potential in the superconducting region will be measured by the chemical potential μ_s. For simplicity, we choose the same effective mass and the same chemical potential in the normal and the superconducting regions in the numerical calculations, but we can show that the results presented below are still valid if the effective mass and the chemical potential in the normal and the superconducting regions are set different, thus we neglect these differences in the following discussion.

From the energy dispersion relations of quasiparticles in the superconducting region, one can see that there is a critical value $B_\mathrm{c}=\sqrt{\Delta^2+\mu_\mathrm{s}^2}$ for the strength of the Zeeman magnetic field, at which a transition from a topologically trivial superconducting state to a topologically nontrivial superconducting state will occur in both 1D and 2D systems. Because the strength of the Zeeman magnetic field is increased from $B_0<B_\mathrm{c}$ to $B_0=B_\mathrm{c}$, accompanied with this topological transition, the interface Andreev bound state will evolve from a non-zero energy bound state to a zero-energy bound state. In Figs. 1(a) and 1(b), we show how the differential shot noise

spectra in 1D and 2D tunnel junctions vary as such an evolution is driven by tuning the strength of the Zeeman magnetic field. From Figs. 1(a) and 1(b), one can see that, for the case of $B_0 = 0$ (no interface bound state emerges in this case), the differential shot noise spectra in both 1D and 2D tunnel junctions exhibit a sharp peak at $eV \simeq \Delta$, similar to the corresponding results for conventional normal-metal/s-wave superconductor tunnel junctions. As B_0 is increased from 0 to B_c, the position of the peak shifts gradually towards zero bias voltage, and the peak height also diminishes gradually. These variations are due to the formation of the midgap interface Andreev bound states and the shifts of their bound energies, which are controlled by varying the strength of the Zeeman magnetic field. From the theoretical point of view, the Andreev reflection process is most pronounced if the energy of an incident electron is close to the bound energy E_b of the interface bound state, thus a midgap peak is formed in the differential shot noise spectrum around the position of $eV \simeq E_b$, and the shift of the peak position can serve as an important indication of the evolution of the interface bound states.

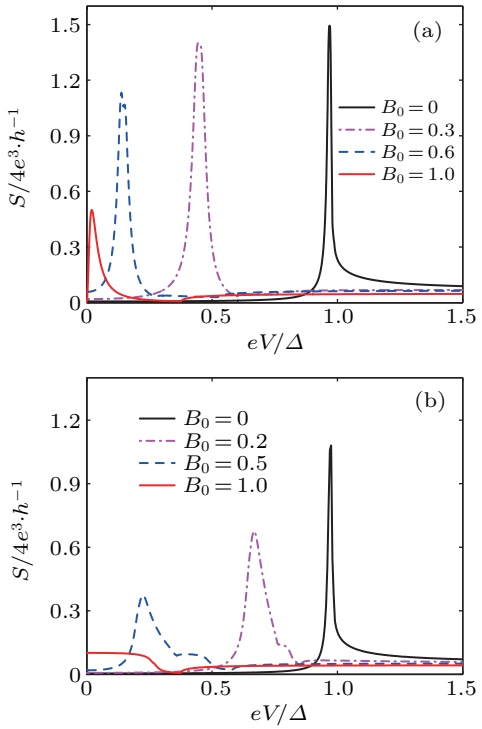


Fig. 1. The differential shot noise in a 1D tunnel junction (a) and in a 2D tunnel junction (b) as a function of the bias voltage for several different strengths of the Zeeman magnetic field. The values of B_0 shown in the figures are given in units of the critical field strength B_c. The other parameters are $\Delta/\mu_s = 0.001$, $\alpha = 0.2$, and $Z_0 = 5$.

By comparing the corresponding results shown in Figs. 1(a) and 1(b), one can see that though the variations of the differential shot noise spectra with the evolution of the interface bound states exhibit some similarities in the 1D and 2D tunnel junctions; however, there are also some significant differences between them. For the 1D tunnel junctions, as B_0 is increased from 0 to B_c, the width of the midgap peak in the differential shot noise spectrum remains rather narrow, i.e., the shot noise remains changing rather rapidly in a narrow bias region around $eV \simeq E_b$, independent of the values of B_0. But for the 2D tunnel junctions, as B_0 is increased from 0 to B_c, the width of the midgap peak will be broadened substantially. Especially, as the value of B_0 is close to the critical value B_c, the variation of the differential shot noise around the peak center becomes rather smooth as compared with the corresponding result for the 1D tunnel junctions. These significant differences are due to the fact that, for the 2D tunnel junctions, the effect of the interface bound states on the normal and the Andreev reflection processes may depend sensitively on the incident angles of the charge carriers.

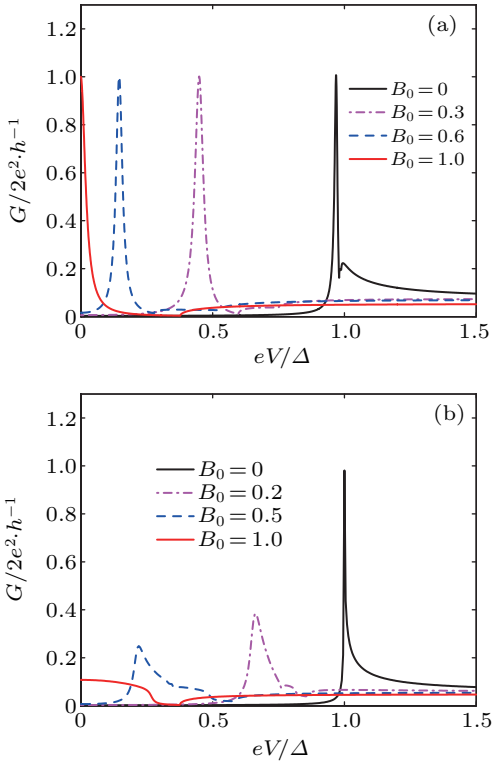


Fig. 2. Illustration of the shift of the midgap conductance peak in the differential tunneling conductance spectrum in a 1D tunnel junction (a) and in a 2D tunnel junction (b) as the strength of the Zeeman magnetic field is increased from $B_0 = 0$ to $B_0 = B_c$. The values of B_0 shown in the figures are given in units of the critical field strength B_c. The other parameters are $\Delta/\mu_s = 0.001$, $\alpha = 0.2$, and $Z_0 = 5$.

In Figs. 2(a) and 2(b), we plot the differential tunneling conductance spectra of both 1D and 2D tunnel junctions as a function of the bias voltage for several different values of the strength of the Zeeman magnetic field. In agreement with the previous theoretical predictions,[11–16] as the strength of the Zeeman magnetic field is increased from $B_0 = 0$ to $B_0 = B_c$, the position of the midgap peak in the differential tunneling conductance spectrum will shift exactly to zero bias voltage as the value of B_0 reaches the critical field strength B_c. These zero-bias conductance peaks (ZBCPs) are responsible for the

formation of zero-energy bound state at the interface in a tunnel junction and were observed in several recent experimental studies.[19–25] By comparing the results shown in Figs. 1 and 2, one can note that, for both 1D and 2D tunnel junctions, as the strength of the Zeeman magnetic field is increased from $B_0 = 0$ to $B_0 = B_c$, the shift of the position of the midgap peak in the differential shot noise spectrum is similar to that in the differential tunneling conductance spectrum. But unlike the differential tunneling conductance spectrum, the position of the midgap peak in the differential shot noise spectrum does not shift exactly to zero bias voltage as the strength of the Zeeman magnetic field reaches the critical value B_c, as can be seen from Fig. 1.

A particularly interesting quantity in noise studies is the ratio of the noise power (P) to the charge current (I).[29–35] In Figs. 3(a) and 3(b), we show the variations of the P/I ratio in both 1D and 2D tunnel junctions as a function of the bias voltage for several different values of the strength of the Zeeman magnetic field. From Fig. 3(a), one can see that, for the case of $B_0 = 0$ (no interface bound state emerges in this case), the P/I ratio in the 1D tunnel junctions is $4e$ in the whole gap region ($eV < \Delta$) and quickly reaches the classical Schottky value $2e$ at finite bias voltages outside the gap region ($eV > \Delta$), similar to the corresponding result for conventional normal-metal/s-wave superconductor tunnel junctions.[29,30] As the strength of the Zeeman magnetic field is increased, the interface Andreev bound state emerges. Due to the induction of the midgap interface bound state, the behaviors of the P/I ratio will deviate significantly from the corresponding results for conventional normal-metal/s-wave superconductor tunnel junctions. The most significant discrepancy is the behaviors of the P/I ratio near zero bias voltage ($eV \ll \Delta$). From Fig. 3(a), one can see that the P/I ratio near zero bias voltage may be increased substantially by the increase of B_0, i.e., the induction of the midgap interface bound state can enhance this ratio significantly in the vicinity of zero bias voltage. But remarkably, as the value of B_0 gets close to the critical field strength B_c, this ratio turns to decrease rapidly with the further increase of B_0 and vanishes completely as the value of B_0 reaches the critical value B_c. This remarkable feature is more clearly illustrated in Fig. 4(a), where we plot the ratio of the zero-bias differential shot noise (S_0) to the zero-bias differential conductivity (G_0) as a function of the strength of the Zeeman magnetic field. In the small bias limit with $eV \ll \Delta$, the P/I ratio is equal to the S_0/G_0 ratio. From Fig. 4(a) one can see that, for small barrier strength (see the curves with $Z_0 = 2$ and $Z_0 = 3$ in Fig. 4(a)), this ratio will increase first with the increase of B_0 and then turn to decrease gradually with the further increase of B_0, but as B_0 reaches the critical field strength B_c, it decreases sharply to zero. For large barrier strength (see the curve with $Z_0 = 5$ in Fig. 4(a)), this ratio will increase with the increase of B_0 almost in the whole region of $B_0 < B_c$, but decreases sharply to zero as the value of B_0 reaches the critical value B_c. Such remarkable feature is an important reflection of the formation of zero-energy interface bound states in the 1D tunnel junctions.

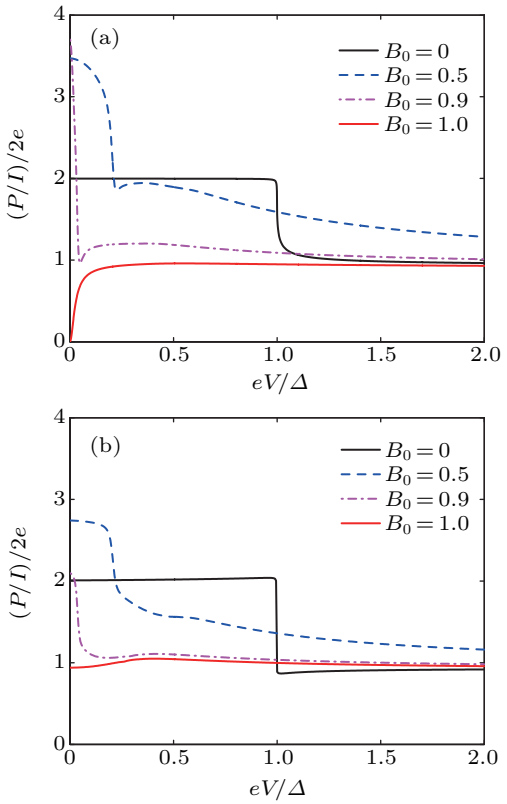


Fig. 3. The ratio of the noise power to the charge current in a 1D tunnel junction (a) and in a 2D tunnel junction (b) as a function of the bias voltage for several different strengths of the Zeeman magnetic field. The values of B_0 shown in the figures are given in units of the critical field strength B_c. The other parameters are $\Delta/\mu_s = 0.001$, $\alpha = 0.2$, and $Z_0 = 5$.

From Fig. 3(b), one can see that, for the 2D tunnel junctions, the behaviors of the P/I ratio with the evolution of the interface bound state are significantly different from the corresponding results shown in Fig. 3(a) for the 1D tunnel junctions and also significantly different from the corresponding results for conventional normal-metal/s-wave superconductor tunnel junctions. As can be seen from Fig. 3(b), for the case of $B_0 = 0$ (no interface bound state emerges), the P/I ratio in the 2D tunnel junctions is also $4e$ in the whole gap region ($eV < \Delta$) and quickly reaches the classical Schottky value $2e$ at finite bias voltages outside the gap region ($eV > \Delta$), similar to the corresponding result shown in Fig. 3(a) for the 1D tunnel junctions and also similar to the corresponding results for conventional normal-metal/s-wave superconductor tunnel junctions. As the value of B_0 is increased and the interface bound state emerges, the P/I ratio near zero bias voltage in the 2D tunneling junction can also be enhanced significantly due to the induction of the midgap interface bound states. But as the value of B_0 gets close to the critical value B_c, the P/I ratio near zero bias

voltage turns to decrease smoothly to a finite value, which is neither zero as the corresponding results shown in Fig. 3(a) for the 1D tunnel junction, nor the usual value $4e$ as in conventional normal-metal/s-wave superconductor tunnel junctions, but recovers approximately the normal-state result $2e$. Such behavior is more clearly illustrated in Fig. 4(b), where we plot the ratio of the zero-bias differential shot noise S_0 to the zero-bias differential conductivity G_0 (equal to the P/I ratio in the small bias limit with $eV \ll \Delta$) in the 2D tunnel junctions as a function of the strength of the Zeeman magnetic field. From Fig. 4(b) one can see that the variation of this ratio with the increase of B_0 is rather smooth in the whole region of $B_0 < B_c$, compared with the corresponding result shown in Fig. 3(a) for the 1D tunnel junctions. These significant differences are due to the fact that the influence of the midgap interface bound state on the normal and Andreev reflections of charge carriers at the interface in a 2D tunnel junction may depend sensitively on their incident angles.

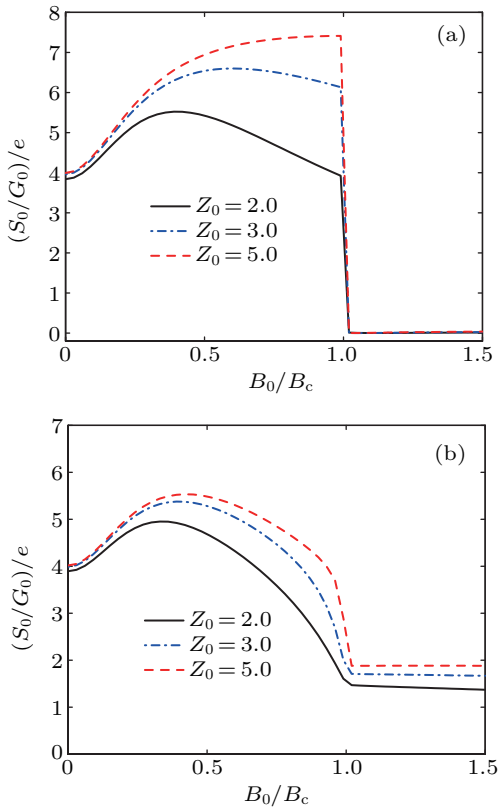


Fig. 4. The ratio of the zero-bias differential shot noise S_0 to the zero-bias differential conductivity G_0 in a 1D tunnel junction (a) and in a 2D tunnel junction (b) as a function of the strength of the Zeeman magnetic field for several different values of the interface barrier strength Z_0. The other parameters are $\Delta/\mu_s = 0.001$ and $\alpha = 0.2$.

4. Conclusion

We have presented a theoretical investigation of the variations of the electrical shot noise properties with the evolution of the midgap interface bound states in tunnel junctions formed between normal metals and 1D or 2D Rashba semiconductors with proximity-induced s-wave pairing potential and Zeeman magnetic field. It is shown that the electrical shot noise properties in these tunnel junctions may deviate significantly from conventional normal-metal/s-wave superconductor tunnel junctions due to the induction of the midgap interface bound state in the gap region. It is found that in both 1D and 2D tunnel junctions, the ratio of the noise power to the electric current in the vicinity of zero bias voltage may be enhanced significantly due to the induction of the midgap interface bound state. But as the interface bound state evolves from a non-zero energy bound state to a zero-energy bound state, this ratio tends to vanish completely at zero bias voltage in the 1D tunnel junctions, while in the 2D tunnel junctions it decreases smoothly to the classical Schottky value $2e$ as in the normal state. This result clarifies an important difference between the properties of zero-energy interface bound states formed in 1D and 2D Rashba semiconductors with proximity-induced s-wave pairing potential and Zeeman magnetic field. Some other important discrepancies between the shot noise properties in 1D and 2D tunnel junctions are also clarified. The theoretical model considered above is suitable for low-dimensional tunnel junctions based on both InSb and InAs nanowires or thin films with proximity-induced superconductivity. We believe that some interesting behaviors of the shot noise predicted above should be observable in these systems, and the observation of these interesting behaviors will be helpful to get more useful information on the properties of anomalous interface bound states formed in such low-dimensional systems, which is not currently available through usual conductance measurements.

References

[1] Linder J and Robinson J W A 2015 *Nat. Phys.* **11** 307
[2] Beckmann D 2016 *J. Phys. C* **28** 163001
[3] Eschrig M 2011 *Physics Today* **64** 43
[4] Jacobsen S H, Kulagina I and Linder J 2016 *Sci. Rep.* **6** 23926
[5] Costa A, Högl P and Fabian J 2017 *Phys. Rev. B* **95** 024514
[6] Espedal C, Yokoyama T and Linder J 2016 *Phys. Rev. Lett.* **116** 127002
[7] Konschelle F, Tokatly I V and Bergeret F S 2015 *Phys. Rev. B* **92** 125443
[8] Amundsen M and Linder J 2017 *Phys. Rev. B* **96** 064508
[9] Bobkova I V and Bobkov A M 2017 *Phys. Rev. B* **95** 184518
[10] Sato M, Takahashi Y and Fujimoto S 2009 *Phys. Rev. Lett.* **103** 020401
[11] Sau J D, Lutchyn R M, Tewari S and Das Sarma S 2010 *Phys. Rev. Lett.* **104** 040502
[12] Alicea J 2010 *Phys. Rev. B* **81** 125318
[13] Lutchyn R M, Sau J D and Das Sarma S 2010 *Phys. Rev. Lett.* **105** 077001
[14] Oreg Y, Refael G and von Oppen F 2010 *Phys. Rev. Lett.* **105** 177002
[15] Stanescu T D, Lutchyn R M and Das Sarma S 2011 *Phys. Rev. B* **84** 144522
[16] Yamakage A, Tanaka Y and Nagaosa N 2012 *Phys. Rev. Lett.* **108** 087003
[17] Ekin J W, Xu Y, Mao S, Venkatesan T, Face D W, Eddy M and Wolf S A 1997 *Phys. Rev. B* **56** 13746
[18] Wagenknecht M, Koelle D, Kleiner R, Graser S, Schopohl N, Chesca B, Tsukada A, Goennenwein S T B and Gross R 2008 *Phys. Rev. Lett.* **100** 227001
[19] Mourik V, Zuo K, Frolov S M, Plissard S R, Bakkers E P A M and Kouwenhoven L P 2012 *Science* **336** 1003

[20] Deng M T, Yu C L, Huang G Y, Larsson M, Caroff P and Xu H Q 2012 *Nano Lett.* **12** 6414
[21] Das A, Ronen Y, Most Y, Oreg Y, Heiblum M and Shtrikman H 2012 *Nat. Phys.* **8** 887
[22] Rokhinson L P, Liu X Y and Furdyna J K 2012 *Nat. Phys.* **8** 795
[23] Finck A D K, Van Harlingen D J, Mohseni P K, Jung K and Li X 2013 *Phys. Rev. Lett.* **110** 126406
[24] Churchill H O H, Fatemi V, Grove-Rasmussen K, Deng M T, Caroff P, Xu H Q and Marcus C M 2013 *Phys. Rev. B* **87** 241401
[25] Chang W, Albrecht S M, Jespersen T S, Kuemmeth F, Krogstrup P, Nygrd J and Marcus C M 2015 *Nat. Nanotechnol.* **10** 232
[26] Stanescu T D and Tewari S 2013 *J. Phys. C* **25** 233201
[27] Roy D, Bondyopadhaya N and Tewari S 2013 *Phys. Rev. B* **88** 020502
[28] Das Sarma S, Nag A and Sau J D 2016 *Phys. Rev. B* **94** 035143
[29] Blanter Y M and Büttiker M 2000 *Phys. Rep.* **336** 1
[30] Anantram M P and Datta S 1996 *Phys. Rev. B* **53** 16390
[31] Tanaka Y, Asai T, Yoshida N, Inoue J and Kashiwaya S 2000 *Phys. Rev. B* **61** 11902
[32] Zhu J X and Ting C S 1999 *Phys. Rev. B* **59** 14165
[33] de Jong M J M and Beenakker C W J 1994 *Phys. Rev. B* **49** 16070
[34] Kane C L and Fisher M P A 1994 *Phys. Rev. Lett.* **72** 724
[35] Landauer R 1993 *Phys. Rev. B* **47** 16427
[36] Liu K, Xia K and Bauer G E W 2012 *Phys. Rev. B* **86** 020408